CAAP Quarterly Report

Date of Report: April 8, 2016

Contract Number: DTPH5615HCAP03

Prepared for: James Prothro, PHMSA-DOT

Project Title: Bayesian Network Inference and Information Fusion for Accurate Pipe Strength and Toughness Estimation

Prepared by: Arizona State University, University of Colorado-Denver

Contact Information: Dr. Yongming Liu and Dr. Yiming Deng

For quarterly period ending: April 10, 2016

Business and Activity Section:

ASU Student training activities

- Sonam Dahire works on the material specimen preparation, testing, and data analysis;
- Sonam Dahire and Tishun Peng work on the Bayesian inference with experimental measurements;
- Ankita Kardile works on the numerical and experimental testing for the ABI testing for strength estimation;
- Sonam Dahire and Ankita Kardile write the report.

CU Denver student training activities

- Xiaodong Shi works on multi-physics modeling, numerical algorithms development and analysis, as well as fast continuous imaging protocol design and implementation
- Salem Egdaire works on NMMI amplitude and phase imaging development Xiaodong Shi and Deepak Kumar works on the experimental testing for data fusion and correlations between electromagnetic measurements and mechanical measurements
- Deepak Kumar works on the compressed sensing assisted fast imaging development
- Xiaodong Shi and Deepak Kumar write the report

(a)Generated Commitments

The system for natural gas pipelines in the United States consists of a network to gather, transport and distribute the product, which consists of 210 systems overall running through the different states. Pipeline infrastructure forms a vital aspect in improving the U.S. economy and standard of living A major portion of the current operational pipelines have been installed in the early 1900's, and therefore lack reliable information on the integrity of the aging pipeline systems which is a critical safety concern. The conventional methods of inspection such as pipeline inspection gauge (PIG) cannot be used to inspect about three-fourth of the present pipeline systems, due to the pipes being too old/ twists/turns etc. which does not allow PIGs to operate in them. In order to maintain the safety and economy standards, accurate estimation of pipe strength and toughness without interrupting the transmission and operations of the pipelines is crucial. Many of the existing techniques focus on single modality measurement for the narrow surface layer measurements and cannot capture decarburization and manufacturing process-induced material inhomogeneity. Also, uncertainties exist in terms of material properties, pipe geometries, manufacturing process, operational conditions, etc., leading to gaps in the accurate strength and toughness determination. Therefore, a novel approach using multimodality diagnosis and information fusion framework has been proposed for probabilistic pipe strength and toughness estimation, which is the objective of the present work. The first part of the project will consist of estimating the basic material properties; microstructure, composition etc. as well as various surface mechanical properties and studying their variation with thickness of the pipeline samples. The second part compromises of advanced testing methods for property estimation with the use of acoustic and electromagnetic sensors. And finally, the information obtained from the two parts would be integrated with the statistical correlations into a multimodal system to obtain a probabilistic strength and toughness with a high degree of accuracy. The typical pipeline grades include A, B, X42, and X46 as distribution pipelines, and X52, X56, X60, X65, X70, X80 etc. for transmission. The latter grades such as X65-X120 have been manufactured through advanced processing methods which imparts a better control on the mechanical properties. However, due to the conventional processing methods for the earlier grades, a large variation in the properties has been observed. These earlier grades still form a vital part of the current service pipelines, hence, a reliable source of information of the aging systems is essential, and therefore form the focus of our study.

Several major tasks are proposed to address the above-mentioned project objectives/goals. Experimental testing, advanced data analysis, numerical simulation, and probabilistic methods are integrated in the proposed tasks. A summary is listed below and detailed work plan will be discussed in the following sections.

Task 1. Experimental testing and data analysis of chemical, metallurgical, and mechanical properties of pipe steel (Arizona State University)

This task focuses on the information obtaining and analysis about the basic pipe steel properties. Both in-house experimental testing and literature data will be used for this task. First, in situ and ex situ chemical composition analysis will be performed for several representative pipe steel specimens (from online vendors and our industry collaborators). Optical emission spectrography (OES) and energy dispersive spectroscopy (EDS) will be used for in situ and ex situ measurements of chemical composition, respectively. Following this, in situ and ex situ pipe steel microstructure analysis will be performed to obtain the grain structure images using etchingbased optical microscopy and electron back scattered diffraction (EBSD) images, respectively. Imaging analysis will be performed to obtain the statistical information and metrics about the pipe steel microstructure, such as grain size distribution. Next, surface hardness measurements will be performed using portable ultrasound hardness testers and the results will be correlated with pipe strength and toughness. Advanced data analysis using Gaussian Process modeling will be used for surrogate modeling and to quantify the uncertainties for future Bayesian network inference.

Task 2. Experimental testing, data analysis and prototyping for acoustic and microelectromagnetic electromagnetic properties of pipe steel (University of Colorado-Denver)

This task focuses on the information obtaining and analysis about the pipe steel acoustic and microelectromagnetic properties. First, ex situ low-frequency near-field microwave microscopy analysis will be performed for several representative pipe steel specimens. Obstacles for dislocation movement, such as grain boundaries and void inclusions, will be revealed in terms of measurable electromagnetic properties. Following that, surface and subsurface microstructural image analysis assisted by Multiphysics modeling will be carried out to understand the correlations between steel strength and different possible mechanisms which impede the dislocation movement under load in the micro electromagnetic spectrum. Next, a prototype of integrating magnetostriction and pulsed eddy current-based Barkhausen noise imaging system will be developed to characterize the pipe steel's Bloch wall jumps and the results will be correlated with pipe strength and toughness experimentally with advanced data analysis.

Task 3. Bayesian network for information fusion and probabilistic pipe strength estimation (Arizona State University and University of Colorado-Denver)

This task will focus on the development of a novel Bayesian network for the inference of pipe strength and toughness. First, the network structure and conditional probability estimation will be performed using the multi-modality diagnosis data obtained in Tasks 1&2. Following this, parametric studies with synthetic data using the developed Bayesian network will be performed to investigate the behavior and performance of the information fusion framework. Sensitivity analysis will be performed to identify the important factors in the proposed Bayesian network. Finally, model verification and validation with realistic

field/laboratory measurements will be demonstrated. Probabilistic pipe strength estimation and associated risk-based confidence determination will be quantified.

A schematic illustration of the proposed components and their integration is shown in Fig.1. The philosophy behind the proposed methodology is that each modality diagnosis will contain part of the information about the pipe steel strength and a fusion process will, in principle, provide more accurate estimation of the current state of the aging pipes. This schematic illustration also indicates the multidisciplinary collaborative work of the proposed study. Mechanical and material research (ASU), electromagnetic and acoustic study (CU-Denver), and industrial experiences (GTI) are integrated together for the probabilistic pipe strength estimation and future decision making for risk mitigation.

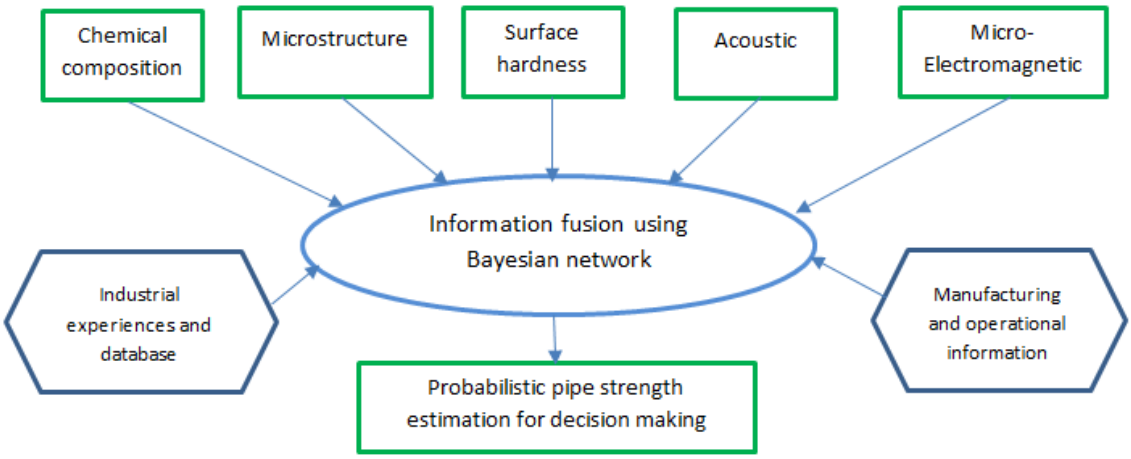

Figure 1.a): Schematic illustration of the proposed pipe strength estimation framework

(b) Status Update of Past Quarter Activities

SECTION 1:

Task 1. Experimental testing and data analysis of chemical, metallurgical, and mechanical properties of pipe steel

Summary

To follow on from the project objective, several literature studies had been carried out as a part of the previous quarterly progress, in order to obtain a better understanding of the present system. The study comprised of investigation of chemical and mechanical properties, such as composition, microstructure, stress-strain behavior etc., for the different grades of linepipe steel, to understand their generic behavior. Next, statistical correlations were obtained between Yield strength and the material basic microstructural and chemical parameters strength, to be used as likelihood functions in the Bayesian network fusion model. And finally, methods for in-situ investigation of the toughness were in development, through the design of an ABI fixture.

In the present review, different experiments were conducted on the linepipe steel samples obtained from GTI, from one particular year of manufacturing. The experimental testing consisted of microstructure examination through Optical/SEM, image analysis through Image J software, composition analysis through EDS and Hardness tests with the Leeb Ball Hardness Tester. In order to study the property variation along the pipe wall thickness, these experiments were conducted at different thicknesses for the specimens. An Ultrasonic thickness gauge was used to verify the thickness, for this purpose. Literature was further investigated to obtain statistical relationship better suited to the system under study. Also, literature has been investigated in order to understand the impact of processing conditions on the microstructure and thereby the mechanical properties. Finally, as a part of the third task, a preliminary Bayesian Network model has been developed to integrate the different components and estimate the probabilistic strength.

Content

Samples from GTI:

The following samples were obtained from GTI, with the information of the installation year. The suspected grade and corresponding microstructures were obtained from the literature, based on the year of installation [1].

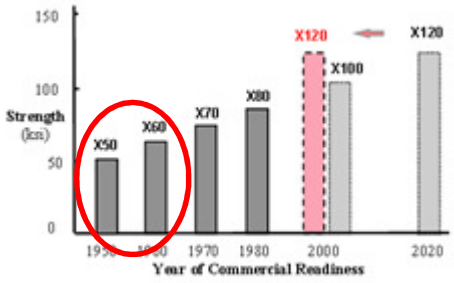

Figure 1b: Development of pipeline steels [1]

***Table1**: Sample Information from GTI:*

Pipe Number	***Installation year***	***Pipe grade***	***Suspected grade***	***Suspected microstructures***
24	*2004*	*1522H*	*X100*	*BAINITE + MARTENSITE or bainite laths and M/A packets*
32	*1958*	*1522H*	*X60-X70*	*FERRITE PEARLITE*
35	*1961*	*1010*	*X60*	*FERRITE PEARLITE*
44	*Unknown*	*1513*		*Unknown*
45	*1949*	*1525*	*X50*	*FERRITE PEARLITE*
47	*1964*	*1025*	*X60*	*FERRITE PEARLITE*

Experimental testing

1. Microstructure Examination:

1. a. Sample Preparation:

a. The sample under investigation was obtained from **Pipe Number 45**. The original pipe was curved with an approximate thickness of 7.8mm with the transverse direction labelled.
b. Flat samples were carved out of the curved pipe; Cross-section -10mm x 10mm, thickness -1mm, 2mm…7mm
c. Samples were polished using Metallographic guidelines on the Silicon carbide papers and diamond cloth for finishing.
d. Thickness gauge was used to verify the sample thickness.
e. Samples were etched in 2% Nital solution for about 10-20 seconds.
f. SEM was used to obtain the microstructures.

1. b.Thickness Gauge Setup:

Figure 2: Thickness gauge set up

2. SEM analysis results:

2.a. Top View Analysis:

a. Sample thickness- 2mm

Figure 3a: Microstructure at 200 X

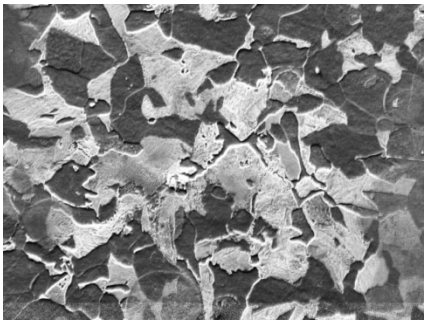

Figure 3b: Microstructure at 700 X

b. Sample thickness- 4mm

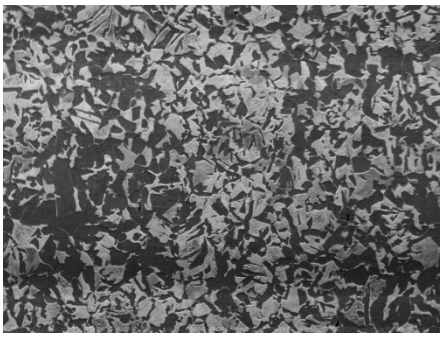

Figure 4a: Microstructure at 200 X

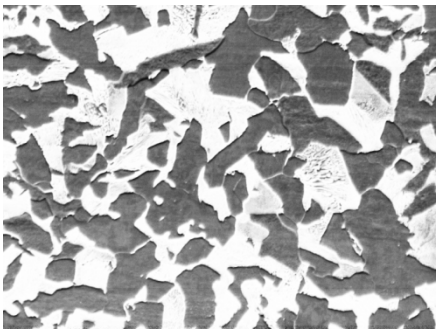

Figure 4b: Microstructure at 700 X

c. Sample thickness- 6mm

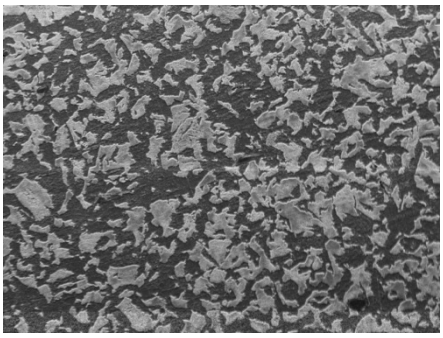

Figure 5 a: Microstructure at 200 X

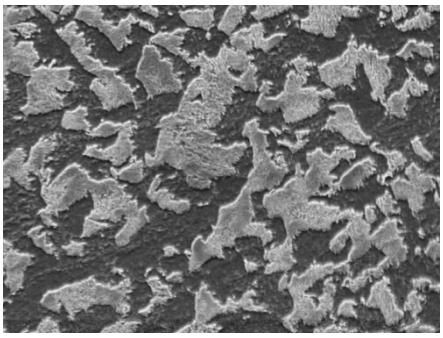

Figure 5b: Microstructure at 700 X

The SEM analysis was conducted on samples at three intermediate thicknesses viz; 2mm, 4mm and 6mm. The preliminary microstructure examination with HITACHI SEM shows the presence of two distinct phases; Ferrite (Dark Constituent) and Pearlite (Light Constituent). Although the grain boundaries are not clearly revealed in the present micrographs, it can be observed that the micrograph corresponding to 4mm thick sample has sharper edges/boundaries, compared to the 2mm and 6mm thick samples.

2.b. Image J analysis:

Image J was used for quantification of area fraction of the two phases in the ferrite/pearlite system, and yields the following results: No significant difference was observed in the phase fraction as per these measurements, the reason for this is still under investigation.

***Table 2**: Quantification of phase percentages*

S.No	Phase	Area Fraction(%)
1	Pearlite	40.897
2	Pearlite	43.899
3	Pearlite	43.651

2.c. Through thickness microstructure analysis:

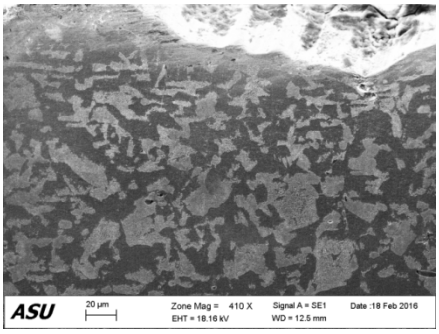

Figure 6a: Edge 1

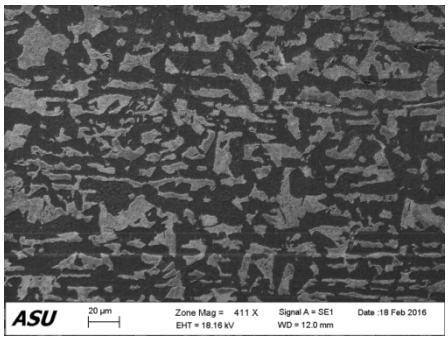

Figure 6b: Edge 2

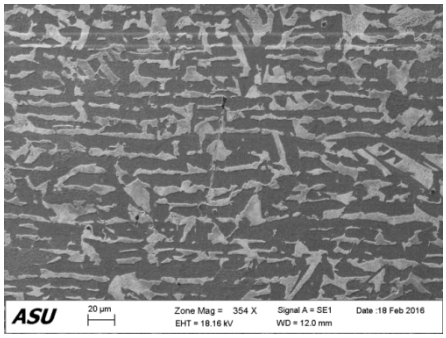

Figure 6c: Edge 3

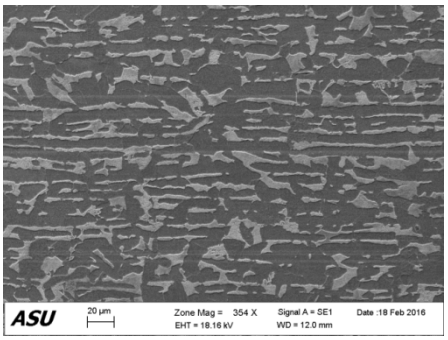

Figure 6d: Edge 4

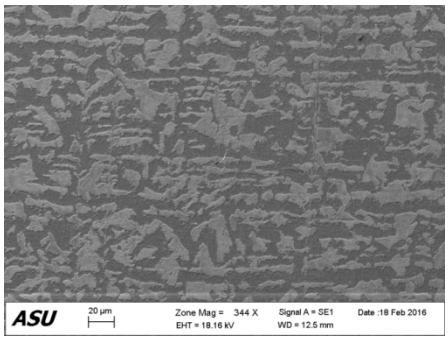

Figure 6e: Edge 5

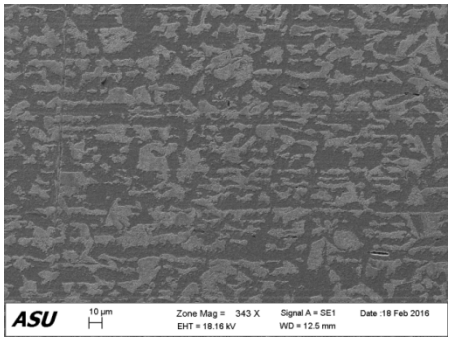

Figure 6f: Edge 6

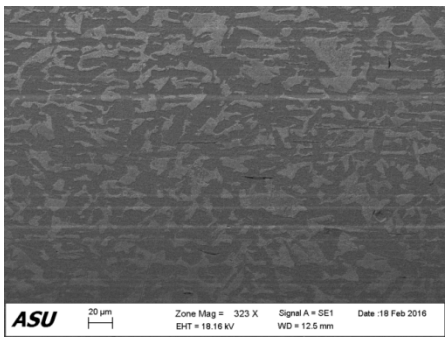

Figure 6g: Edge 7

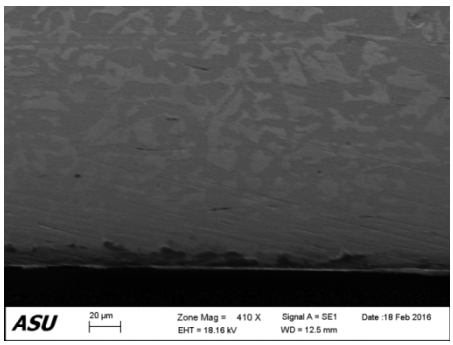

Figure 6h: Edge 8

Samples were also investigated along the pipe wall thickness direction by direct observation of the thickness side (perpendicular to the top view of the specimens). Figures 6a- 6h reveal the microstructures starting from one edge of the sample (top edge) scanned through the other edge (bottom edge). As the sample is traverses along the thickness, it can be seen that the micrographs in the middle region (figure 6d- 6f) depict a certain texture i.e the phases are elongated along one direction (transverse). Some literatures have predicted similar trends which are attributed to be primarily because of the cooling rate. But in these cases, usually the surface micrographs develop a texture due to fast cooling, in contrast to the present scenario. It is therefore, hard to say at the present moment, as to what may be the exact cause to generate such a trend for the system under study.

3. Hardness Test:

The **Leeb Ball Hardness Tester** was used to examine the hardness of the samples, in order to determine the surface variation of hardness.

***Table 3**: Hardness measurements*

Samples Thickness (mm)	Hardness (HV) H1	Hardness (HV) H2	Hardness (HV) H3	Mean Hardness (HV)
2	138	182	161	160.33
4	237	223	234	231.33
6	203	191	181	191.67

As can be seen clearly, the hardness of the samples in the middle region, with sharper phase morphologies, is higher, compared to the surface region of either edge. This can also be considered in line with the region exhibiting a certain texture, which presumably imparts a high value of hardness, or even corresponding higher value for strengths.

Figure 7a: Hardness tester

Figure 7b: Testing setup

4. EDS Analysis:

In order to obtain the chemical composition of the pipeline segment, EDS was conducted on the 4mm thick sample, with the use of XL-30 microscope with an EDS provision. It was observed that the EDS signal could only pick up two-three elements, viz; Fe, S and Mn. None of the other peaks were observed in the EDS spectrum.

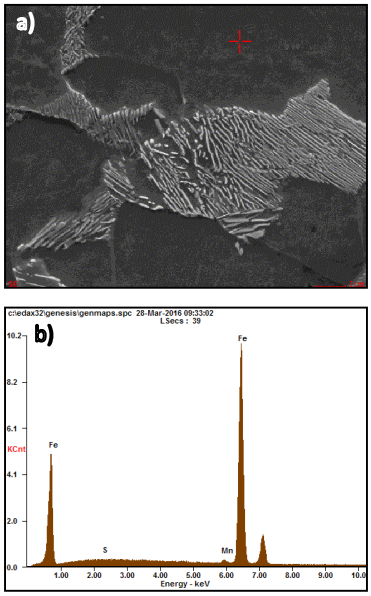

c)

Element	Wt%	At%
SK	00.18	00.32
MnK		01.31
FeK	98.52	98.37
Matrix	Correction	ZAF

Figure 8.1: a) Spot analysis region b) EDS Spectrum c) Elemental Wt%

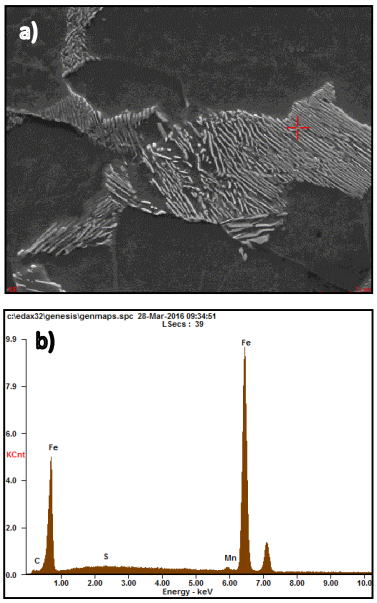

c)

Element	Wt%	At%
MnK	01.22	01.12
FeK	95.69	86.00
Matrix	Correction	ZAF

Figure 8.2: a) Spot analysis region b) EDS Spectrum c) Elemental Wt%

Spot analysis at two different spots (ferrite and pearlite region) show no trace of any elements with a low concentration. This could be due to the noise factor being too high to pick up any elements with a Wt% lower than 0.15. As this technique may not be sensitive enough to resolve the accurate elemental composition, especially Carbon, the next step is move to Electron energy loss spectroscopy (EELS), known to have capabilities of even working with weak signals, and is a widely used technique for Carbon detection.

Task 3. Bayesian network for information fusion and probabilistic pipe strength estimation

A preliminary Bayesian Network model has been developed with the use of an open source software WINBUGS, for probabilistic yield strength prediction. This is based on the general Bayes theorem [2]:

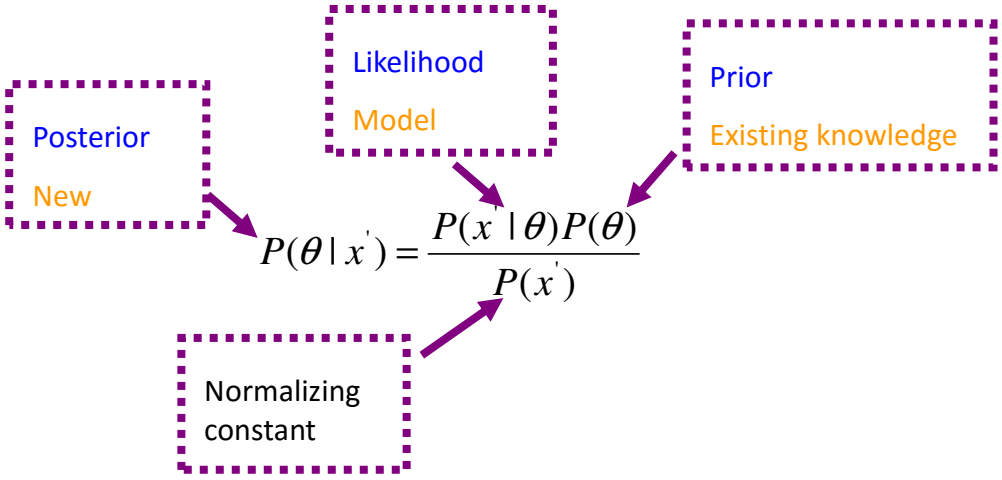

The model was developed step by step by increasing the strength dependence of the Nodes.

The minimum yield strength of API X 52 pipes is typically around 360 MPa.

The first such model is just based on the statistical relationship between yield strength and hardness:

YS=2* H+105 [3], where H - Vickers hardness

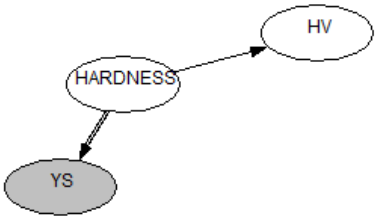

Figure 9a: YS and Hardness BN Model

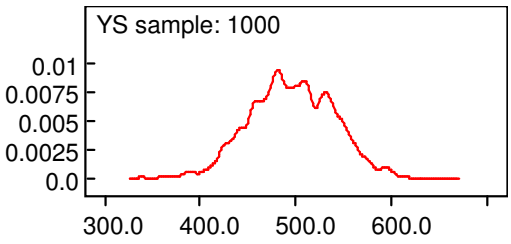

Figure 9b: pdf(YS) vs YS(MPa)

Here, HV is measurement node used to update the node Hardness, which is a stochastic node with normal distribution, similar to HV. The mean value, as can be seen is observed to be 496.0 MPa with a standard deviation of 45.24

The second model is based on adding nodes to account for the impact of microstructural feature such as grain size and compositional parameters, for a ferrite/ pearlite steel type:

YS= 53.9 + 32.34(Mn) +83.2(Si) +354.2(N_f) + 17.4 ($d^{-1/2}$) [4]

where Mn – Mn content (%), Si – Si content (%), Nf - free N content (%), and d -ferrite grain size (in mm)

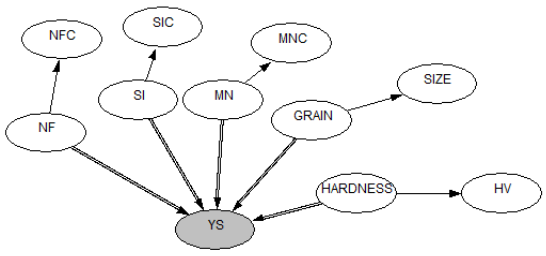

Figure 10a: YS and Hardness-grain size-composition BN Model

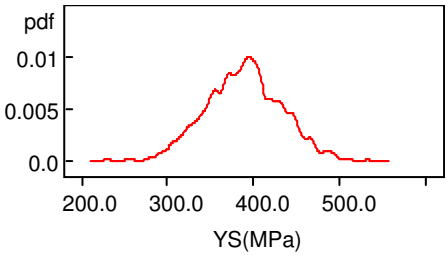

Figure 10b: pdf(YS) vs YS(MPa)

The nodes NFC, SIC,MNC, SIZE and HV are again used to update the nodes NF (free nitrogen content), SI (Si Content), MN (Mn content), GRAIN (Ferritic Grain Size), Hardness (Vickers Hardness). All the a stochastic nodes are designed with a normal distribution. The corresponding

predicted Yield Strength is 388.8 MPa with a standard deviation of 45.51, which is closer to the typical value for these types of steels, marking convergence in the system.

The third updated model also accounts for the dependence of yield strength on the volume fraction of the phases, based on the following generic relationship:

$YS_{(f/p)=} YS_{(f)} (V_f) + YS_{(p)} (1-V_f)$ [5],

Where $YS_{(f/p)}$ is the yield strength of the dual phase material, $YS_{(f)}$ is the yield strength of the ferritic phase and $YS_{(p)}$ is the yield strength of the pearlite phase. V_f is the volume fraction of ferrite.

The Yield Strength of the two phases can be determined from known literature sources [6]

The values for YS for ferrite and pearlite used here are 474.2 MPa and 663.4 Mpa.

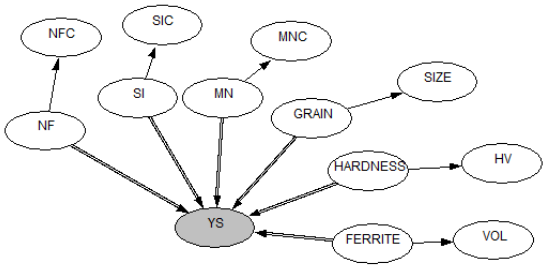

Figure 11a: YS and Hardness-grain size-composition- phase volume BN Model

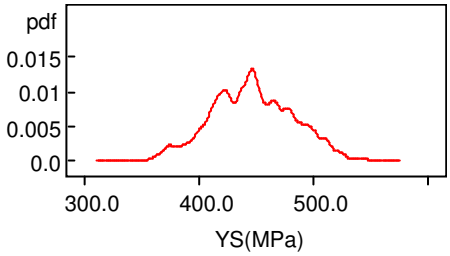

Figure 11b: pdf(YS) vs YS(MPa)

The additional node FERRITE in this case refers to the volume fraction of ferrite phase. The node VOL is used to update the value for the same, and they follow normal distributions. All the other nodes have the same meaning as above. The predicted mean for the YS in this case is 447.5 MPa and standard deviation is 36.44. This signifies the different weights have to be assigned to the different nodes, with a series of training data, in order to obtain better convergence, which is the next step in the analysis.

References:

1. J.Y.Koo,M.J.Luton,M.V.Bangan,R.A.Petkovi. Metallurgical Design of ultra-Strength steel for Gas pipeline.
2. Liu, W., K. Yue, and J. Zhang, Augmenting learning function to Bayesian network inferences with maximum likelihood parameters. Expert Systems with Applications, 2009. **36**(2, Part 2): p. 3497-3504
3. S.H. Hashemi (2010). Strength–hardness statistical correlation in API X65 steel, *Materials Science and Engineering A 528 (2011) 1648–1655*
4. Bruce L. Bramfitt (1998). Structure/Property Relationships in Irons and Steel, *Bethlehem Steel Corporation. ASM International.*

5. Zhonghua Li a, S. Schmauder b, M. Dong b. A simple mechanical model to predict fracture and yield strengths of particulate two-phase materials. *Computational Materials Science 15 (1999) 11-21*
6. Thomas Hoper.Shigeru Endo.Nobuyuki Ihikawa and Koichi Osawa (1999). Effect of Volume Fraction of Constituent phases on the stress-strain relationship of Dual Phase Steels. *ISIJ International, Vol. 39.*

Planned activities for the next quarter:

1. To investigate the trend in the microstructure behavior along the pipe wall thickness and the contributing factors.
2. To conduct EBSD on the samples to inspect for any trend in the crystallographic orientations.
3. To conduct a revised EDS study and EELS analysis for composition determination.
4. To improve the Bayesian Network Model by providing additional training data to obtain better convergence.
5. To further extend the Bayesian Network Model for YS prediction, to predict the tensile strength, fracture toughness etc.
6. To extend the experiments to other samples.

SECTION 2:

Design of Automated Ball Indentation test equipment:

Summary

The United States transports liquid petroleum over 190,000 miles whereas the natural gas pipeline system is a massive underground network of over 2.4 million miles [1]. About 67% of the total crude oil pipelines were laid down before 1980 [2]. Hence, on an average, the age of the pipes currently in use is approximately 35 years in service. Over a period of time, due to the internal as well as external conditions of the pipelines, they deteriorate gradually. Corrosion is the main cause for deterioration of the pipelines. The integrity of the pipeline is important to avoid leakage, leading to safety and environmental hazards and tremendous losses. Of the hazardous liquid pipeline accidents caused by corrosion, 65% were due to external corrosion and 34% were due to internal corrosion. For, natural gas transmission pipeline accidents, 36% were caused by external corrosion and 63% were caused by internal corrosion [3]. Thus, testing of pipelines for its material properties and strength has become of prime importance. Conventional mechanical tests require a large amount of test material and in most of the cases this may not be available from the components that are in service. Therefore, it is of great importance to develop methods which can be performed in-situ. Since the testing is carried out in-situ, it needs to be non-destructive or minimally destructive in order to serve the purpose of testing [4]. The automated ball indentation (ABI) test is based on strain-controlled multiple indentations (at the same penetration location) of a polished surface by a spherical indenter (0.25 to 1.57-mm diameter). The microprobe system and test methods are based on well demonstrated and accepted physical and mathematical relationships which govern metal behaviour under multiaxial indentation loading [5].

The objective of the research project is to determine the through thickness mechanical properties (toughness, yield strength, ultimate tensile strength etc.) of a material specimen using ABI testing. An electromechanical MTS testing machine, capable of a maximum loading of 10kN is being used to carry out the ABI testing. To fit the indenter in the machine, a fixture has been designed for the top head of the machine. Another fixture has been designed for the bottom head to hold the testing specimen in place. The displacement and load of the indenter can be monitored on a computer connected to the machine. Simulation for the loading of the indenter on a steel test specimen is being carried out using ABAQUS. A MATLAB code to process the experimental data in order to obtain the stress-strain curve has been written.

1. Modelling:

The geometry of the indenter and plate is modelled in ABAQUS as shown in Figure 1, where the indenter is considered to be a analytical rigid body, given its high hardness and the plate material is considered to be steel with elastic-plastic deformation occurring due to the contact. The material properties used for the steel plate are summarized as given below:
Modulus of Elasticity – 210.7GPa
Poisson's Ratio – 0.303

Yield stress (MPa)	Plastic Strain
200.2	0
246	0.02353
294	0.0474
374	0.09354
437	0.1377
480	0.18

Table 1. Plastic properties for steel

Boundary conditions are applied on the plate and indenter so as to simulate the contact of the pair. The bottom face of the plate was fixed and the load is applied on the top face of the indenter. The boundary conditions applied are shown in Figure 2. While defining the contact pair, the plate is made the master surface whereas the indenter is considered as the slave surface.

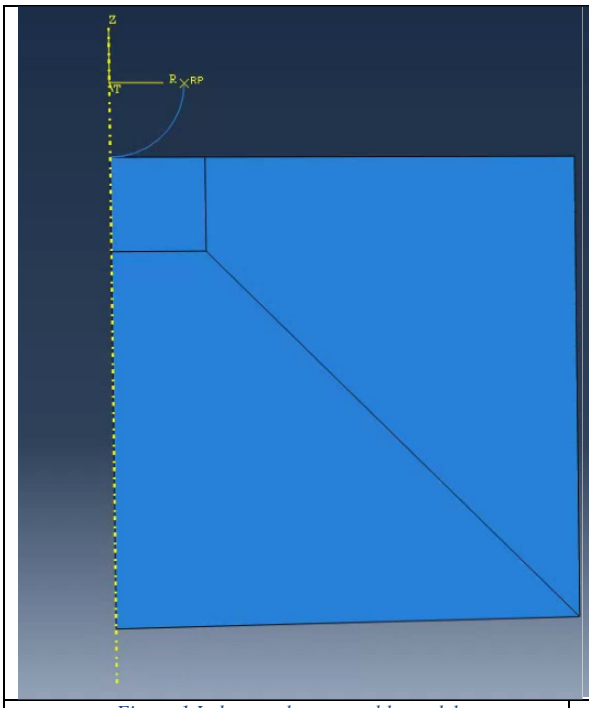

Figure 1 Indenter-plate assembly model

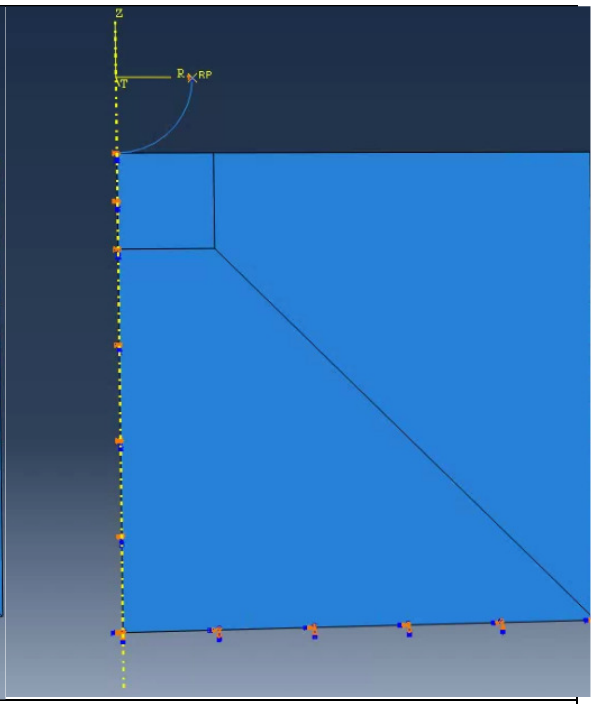

Figure 2 BC and loading of assembly

The model was meshed using various control parameters such as edge divisions to achieve good quality elements in the desired region. Previously, a 3D case of the geometry was considered for analysis. However, the convergence of the system becomes difficult due to the nature of the geometry of indenter and the distortion of elements near the contact region.

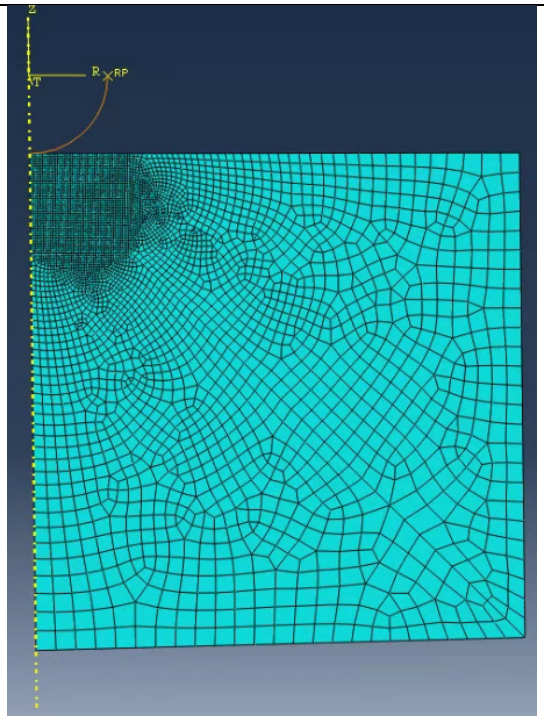

Figure 3 Meshed model of assembly

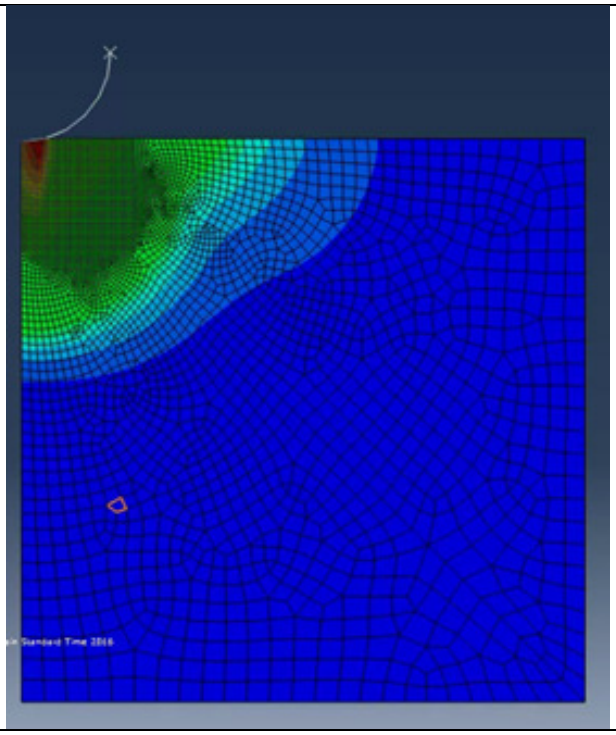

Figure 4 stress contour for a single loading case

A 2D axisymmetric case was considered for simulation where the indenter was modelled as an analytical rigid body. The loading cases and results can be seen in Figure 3 and Figure 4.

2. Code to post-process experimental data:

A code was written to translate the load-displacement curve to the stress-strain curve. The equations are developed from the geometry of the indenter and the indentation on the test specimen [5]. The system of non-linear equations which need to be solved in order to obtain the true stress and strain from the load and displacement can be given as shown in figure:

$$\varepsilon_p = 0.2\, d_p / D$$

$$\sigma_t = 4P / \pi d_p^2 \delta$$

where

$$d_p = \{0.5CD[h_p^2 + (d_p/2)^2]/[h_p^2 + (d_p/2)^2 - h_p D]\}^{1/3}$$

$$C = 5.47P(1/E_1 + 1/E_2)$$

$$\delta = \begin{cases} 1.12 & \Phi \le 1 \\ 1.12 + \tau \ln \Phi & 1 < \Phi \le 27 \\ \delta_{\max} & \Phi > 27 \end{cases}$$

$$\Phi = \varepsilon_p E_2 / 0.43\sigma_t$$

$$\delta_{\max} = 2.87\alpha_m$$

$$\tau = (\delta_{\max} - 1.12)/ln(27)$$

Figure 5 system of non-linear equations which need to be solved [5]

The notations given in the figure above represent the quantities as given below:

ε_p = true plastic strain induced in the test specimen

d_p = plastic deformation diameter

h_p = plastic deformation height

D = indenter diameter

P = load

δ = parameter whose value depends on the stage of development of the plastic zone beneath the indenter

Φ = indentation variable

E1 = Young's modulus of the indenter material

E2 = Young's modulus of test specimen material

α = constraint factor index

σ_t = true stress

The code was tested using load-displacement values from literature. The assumptions made while formulating the problem in MATLAB are as follows:

1. Young's modulus for both indenter (E = 600*10^3 MPa) and test specimen (193*10^3 MPa)
2. Constraint factor index (0.03-2.6)

The stress strain plots obtained from the method followed above are shown in figure below.

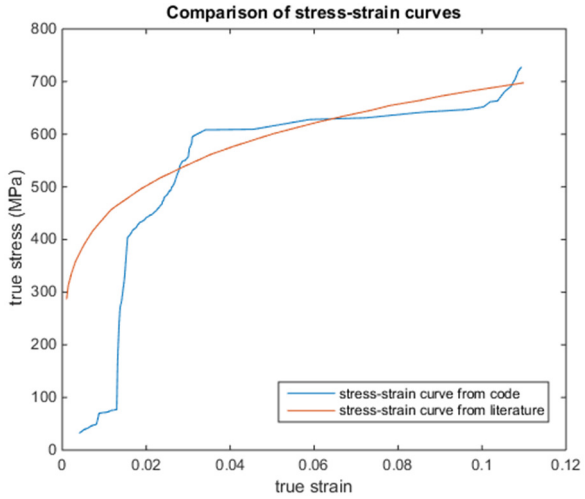

Figure 6 Comparison of stress-strain plot from literature with the coded MATLAB plot

There is a difference in the nature of graph due to various factors such as assumptions taken into consideration, the plot obtained from the code is not curve fitted as opposed to the one taken from literature and the fine tuning of certain material properties.

References:

1. American Petroleum Institute: http://www.americanpetroleuminstitute.com/Oil-and-Natural Gas-Overview/Transporting-Oil-and-Natural-Gas/Pipeline
2. Inside Energy: http://insideenergy.org/2014/08/01/half-century-old-pipelines-carry-oil-and-gas-load/
3. ASME: http://www.asminternational.org/documents/10192/1849770/ACFAB96.pdf
4. Das, M., Pal, T. K., and Das, G., 2012, "Use of Portable Automated Ball Indentation System to Evaluate Mechanical Properties of Steel Pipes," Trans. Indian Inst. Met., **65**(2), pp. 197–203.
5. Haggag, F. M., 1993, "In-situ measurements of mechanical properties using novel automated ball indentation system," ASTM Spec. Tech. Publ., pp. 27–44.

SECTION 3: Task 2. Experimental testing, data analysis and prototyping for acoustic and micro-electromagnetic properties of pipe steel

In the 2nd quarter, CU team continued to develop the micro-electromagnetic sensing prototype as proposed in the project. The sensor development effort was assisted by the 3D numerical simulation as well as the fast imaging research using innovative continuous data acquisition and compressed sensing techniques, which will be summarized in this section.

Task 2.1 Fast imaging acquisition for sensor optimization

Near-field microwave microscopic imaging (NMMI) method is a very useful sensing technique which based on the contrast in electromagnetic properties of the media. It able to providing desirable diagnostic capabilities for applications in several areas. However, Speed is an issue of current single sensor imaging. The initial scanning time for a small area is still very long. A scan of 190 mm x 100 mm area with step size 0.635 mm will cover 48,000 spatial locations. The scanning system applies step by step scanning method will stop at each spatial location and calculate spatial value by averaging 3000 samples. Therefore, to complete an entire scan the system will stop 48,000 times and process 144 million samples during the scanning. It will result in a very long operating time. Another disadvantage of step by step scanning system is the strong. Step by step scanning system repeats moving and stop at each spatial location and introduce vibration and result in inaccuracy.

For a better scan speed and performance, a continuous scanning method which avoid disadvantages mentioned above is under development. In the continuous scanning system, motor will continuous moving until reach the end of each column instead of stop at each spatial location.

In this quarter, we continued to investigate this fast imaging protocol for the proposed micro-electromagnetic sensing methods. Step by step scanning system repeats moving and stop at each spatial location, which is not only time consuming but also introducing vibration during the collecting of data and results in inaccuracy. The continuous scanning method can avoid disadvantages mentioned above and get a better scan speed and performance. Since the motor will only stop when antenna reach the end of the sample, the scanning process is faster and more smooth. In order to reduce the effect of the vibration at each end, the system will sleep 0.5 second before next move. Although sleep function is introduced to the system, the continuous method takes only about 5 minutes for this entire 2x2 square inches scan, which is six times faster than the step by step scanning system.

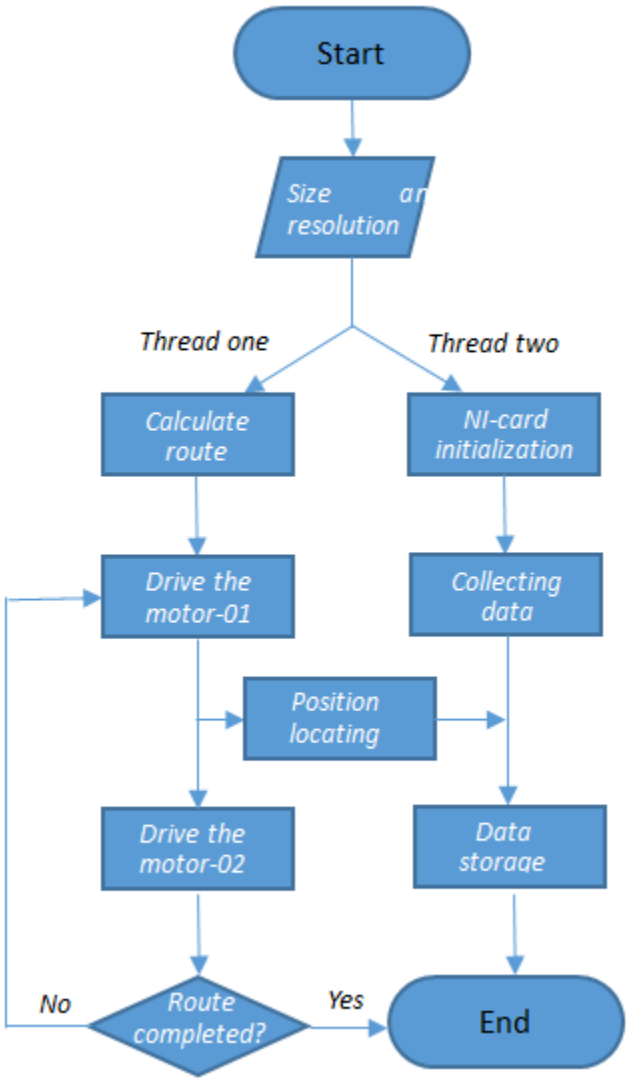

Fig. 2.1. Flow chart of the two thread.

In order to study the noise in the image, we repeat scanning same line for 10 times and study the distribution of the data. The first four scan results of the same line is shown in the following picture. The sampling frequency is 100 KHz.

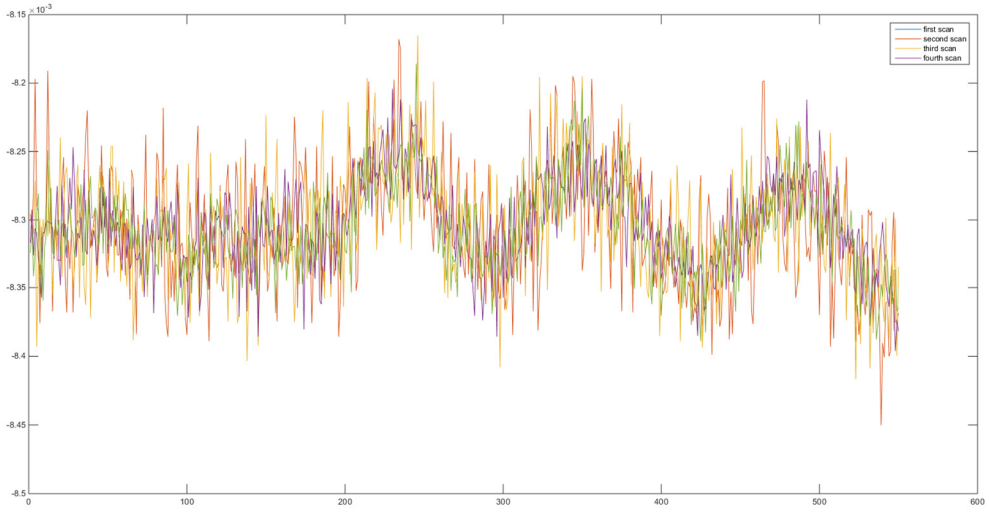

Fig. 2.2 Four scan results of the same line at sample frequency 100 KHz

As we can see in the picture, although we are scanning same line, there are some difference between the data from each scan due to the noise. The variance of 10 results is 1.4846×10^{-5}. In order to get a better result, higher sampling frequency of data receiver have been test. We repeat scanning same line for another 10 times with sampling frequency 200 KHz. Sampling frequency of data receiver will not affect the scanning time but increase the data we collecting.

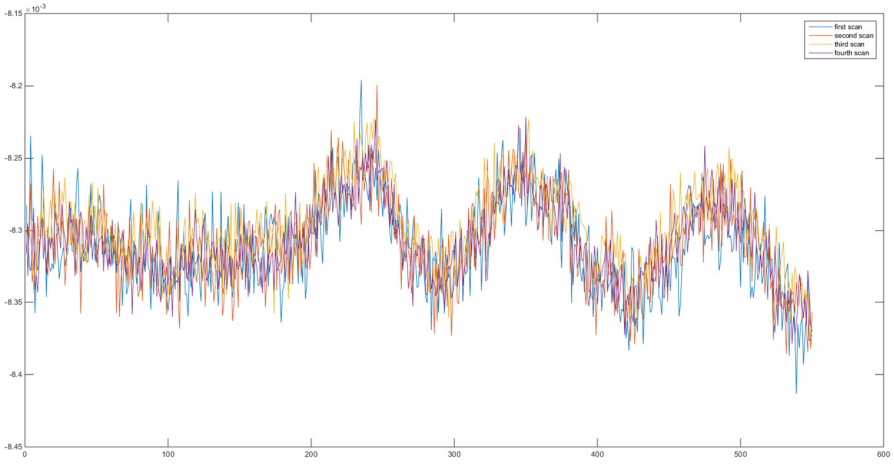

Fig. 2.3. Four scan results of the same line at sample frequency 200 KHz

As picture shown above, the difference between each scan becomes smaller. The variance of 10 results is 5.0845×10^{-6}. Therefore, increase the sampling frequency able to increase signal to noise ratio.

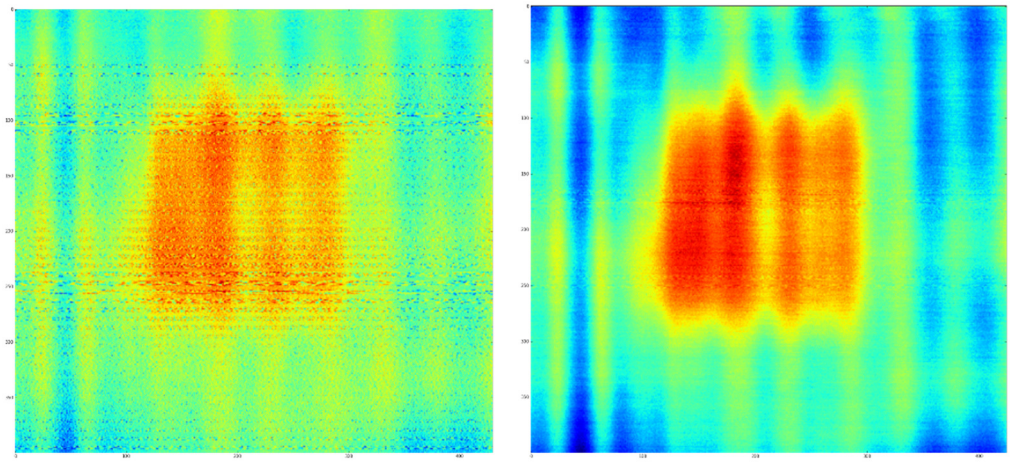

(a) (b)

Fig.2.4 Compare of scanning result with different sampling frequency: (a) 100 KHz and (b) 200 KHz

Since system keeps collecting the data when the motor moving along each line, the data system collected for each line depends on the speed of the motor and sampling frequency of receiver. Therefore, if we want to increase the speed of the motor to improve the speed of the scanning system, we should also increase the sampling frequency to get enough number of data.

Task 2.2 Correlation analysis and data fusion between DIC (mechanical properties) and NMMI (micro-electromagnetic properties)

In order to get a better understanding of correlation between near field result and mechanical test, a mechanical model had been simulated.

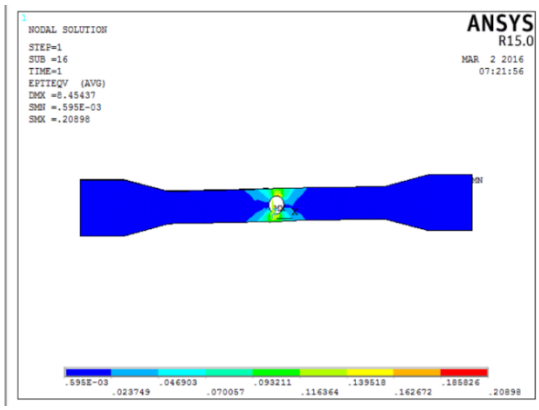

NS_0.7 von Mises strain

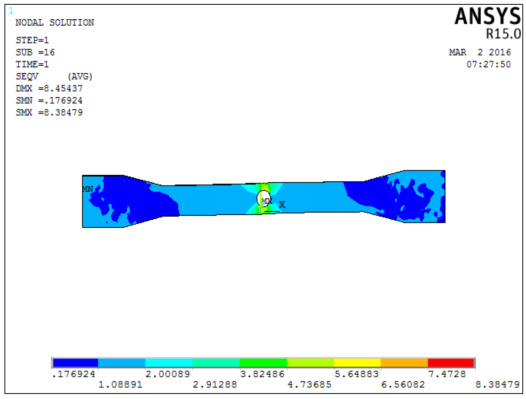

NS_0.7 von Mises stress

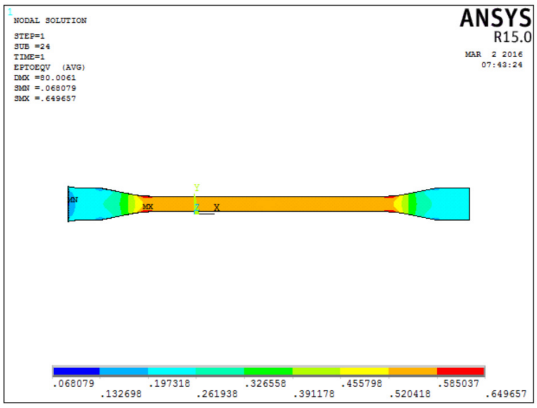

FS_0.7 von Mises strain

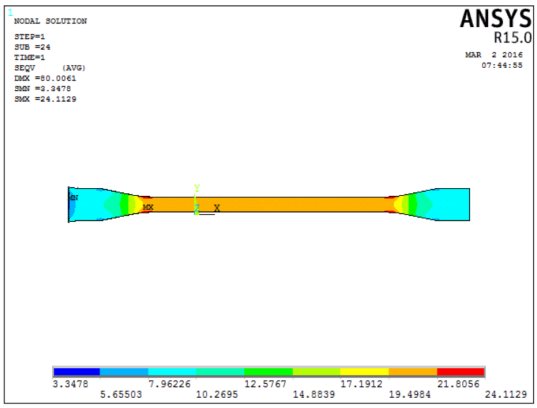

FS_0.7 von Mises stress

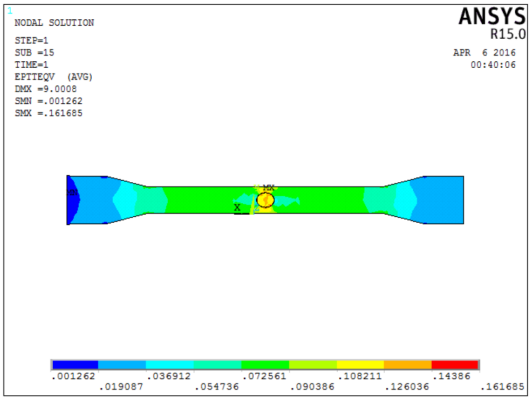

NS_0.3 von Mises strain

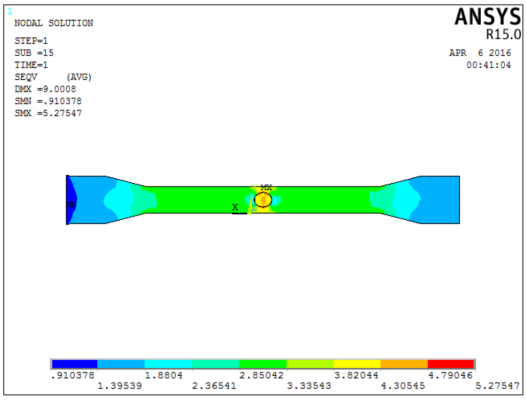

NS_0.3 von Mises stress

Fig. 2.5 von Mises strain and stress simulation

FS is short for full specimen, which means there is no hole on the specimen. NS is short for notched specimen, there is a small round hole on middle of the specimen. 0.7 stands for the percentage of maximum value of displacement when specimens are elongated. For example, if specimen is about to fracture when displacement is 5 cm, 0.7 means specimens are stretched to 3.5 cm.

For the NS specimens, we select section line along the hold root. The 1-D plots of the Von Mises strain have been shown below. As we can see in the picture, the strain reach its peak at the center, where is the location of the hole root. The strength of structure is less then rest part of the specimen due to the hole.

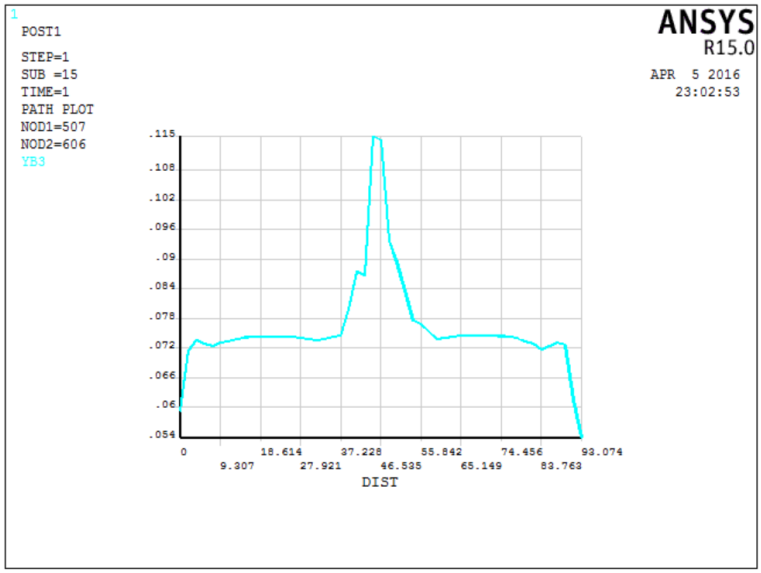

(a) NS_03

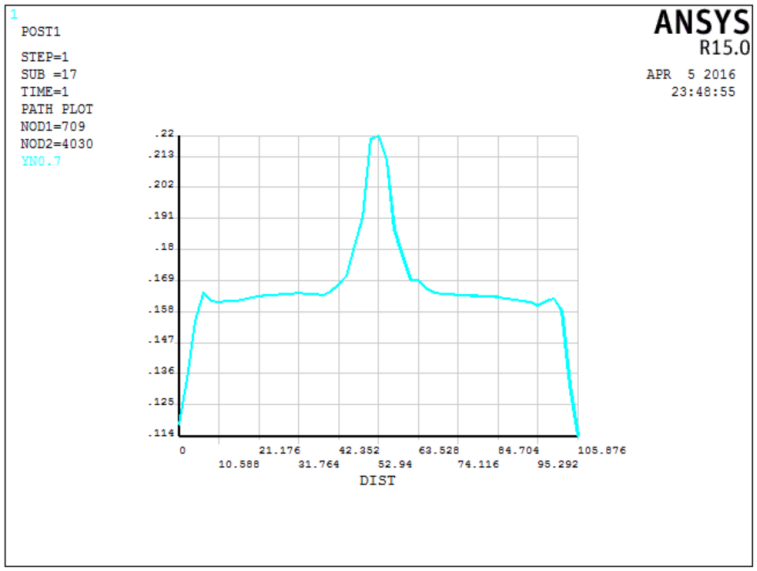

(b) NS_07

Fig.2.6 1-D plot of the von Mises strain

Then we conducted the multi-physics simulation. Use the output of the mechanical simulation as the input of e-field simulation. We select section line along the hold root. The 1-D plots of the E-field have been shown below.

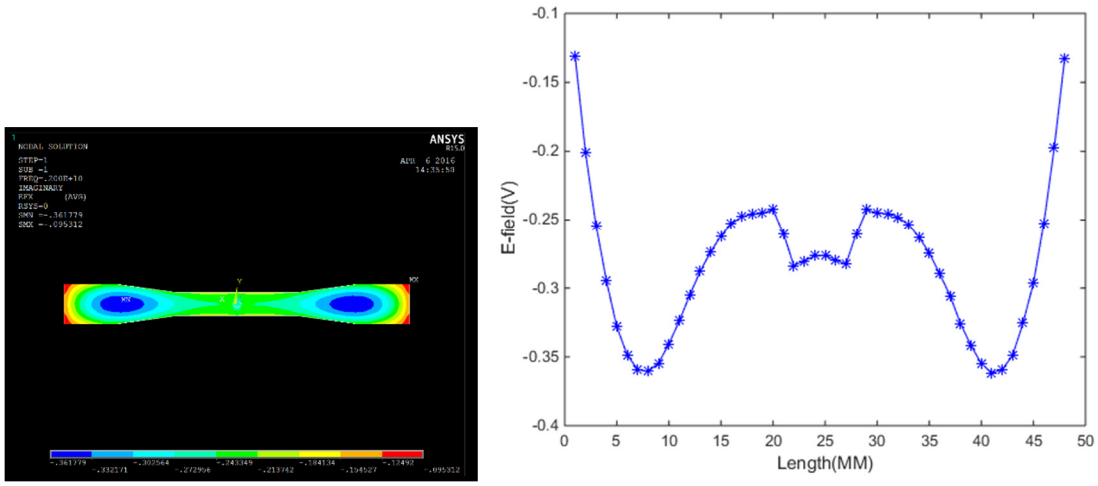

Fig.2.7. Multi-physics simulation of the E- field on the specimen

ASU did tensile testing on the full specimens and notched specimens. We scanned the specimens by nonstop scanning system, in order to compare and correlate the DIC

(mechanical properties) and NMMI (micro-electromagnetic properties). The blue stars stands for the data from near field scanning, and the red dash line is the average of scanning data. The solid blue line is the DIC result.

For the notched specimens, we can see that both of the red lines and blue lines are similar to the simulation result. The trends of red lines and blue lines are similar except the middle part where the hole located.

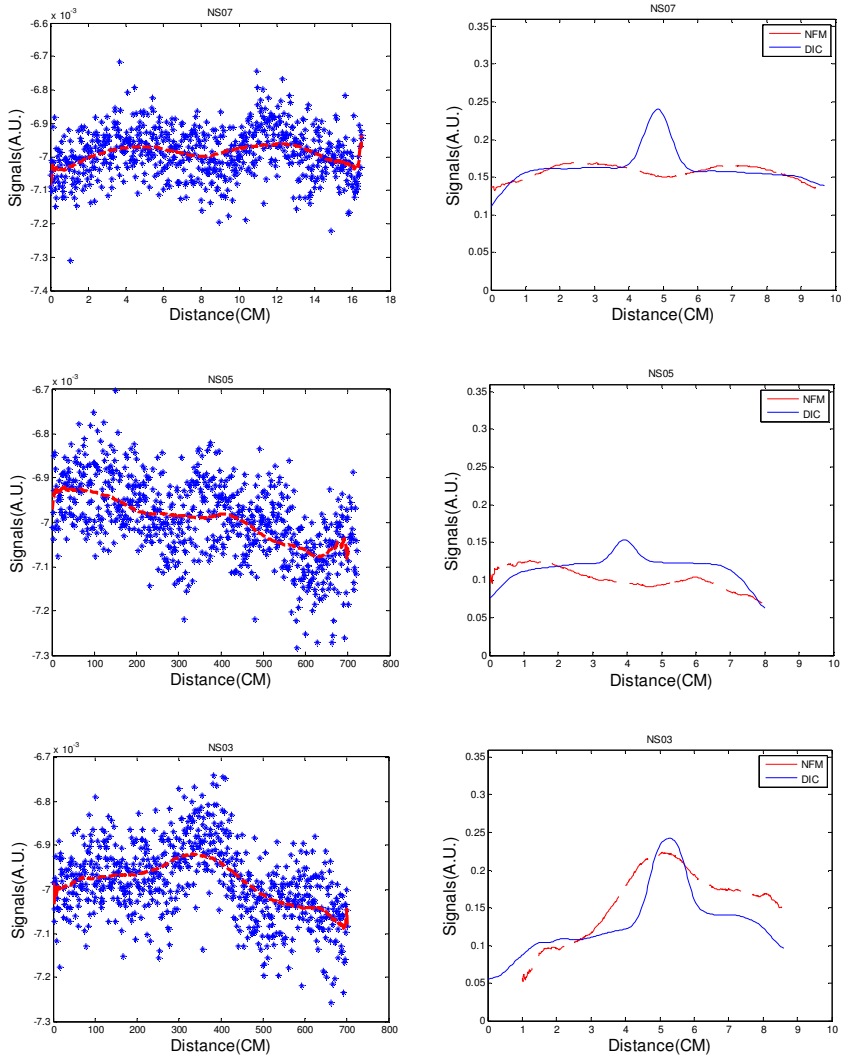

Fig.2.8. scanning results and correlation of the notched specimens

For the full specimens, we can see the trends of the red lines and blue lines are similar. They matched best in FS07 and they matched better in FS05 than FS03.

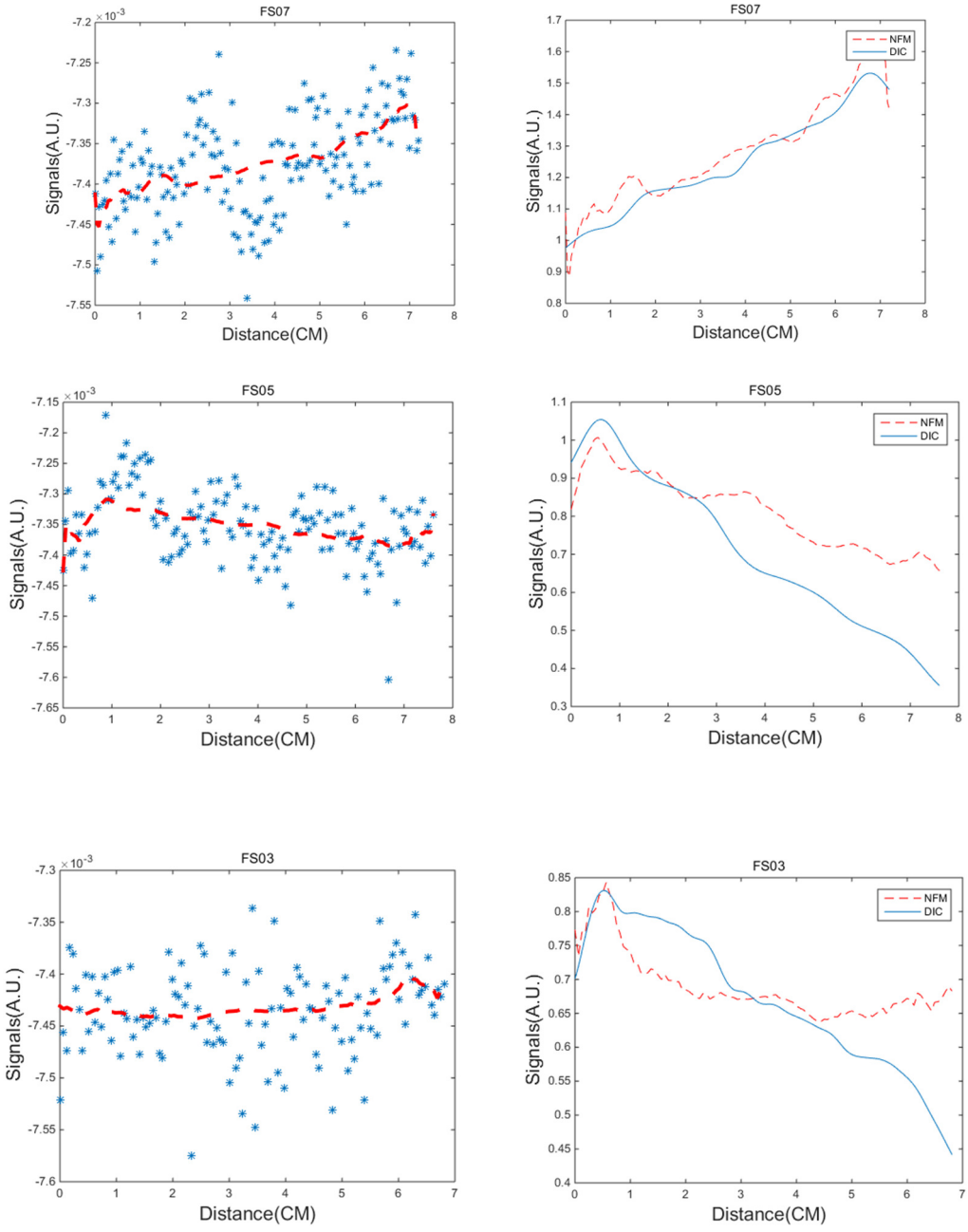

Fig.2.9. scanning results and correlation of the full specimens

For the both full and notched specimens, specimens with larger displacement have a better match result. More specimens will be tested to find the Correlations between DIC and NFMW.

Task 2.3 Compressive sensing based NMMI

Compressive sensing technique, which is the efficient way for signal acquisition is applied to the LEAP's microwave imaging experiment and will be investigated to improve the imaging efficiency for the proposed micro-electromagnetic sensing system. According to the compressive sensing, the original signal be recovered from under sampled data points, by modeling the sampling problem into the underdetermined system of non-linear equations with some prior knowledge of original signal. The prior knowledge for microwave signal is that it shows sparsity in DCT domain. So, the problem can be solved by minimizing the system of non-linear equations using any of the minimization algorithms like basis pursuit, orthogonal matching pursuit, etc.

For this CAAP15 project, CU team has successfully applied the orthogonal matching pursuit (OMP) for solving the underdetermined system of equations [1]. We acquired just the 50% of original signal shown in Fig.2.10 and able to reconstruct the original signal back shown in Fig.2.11.

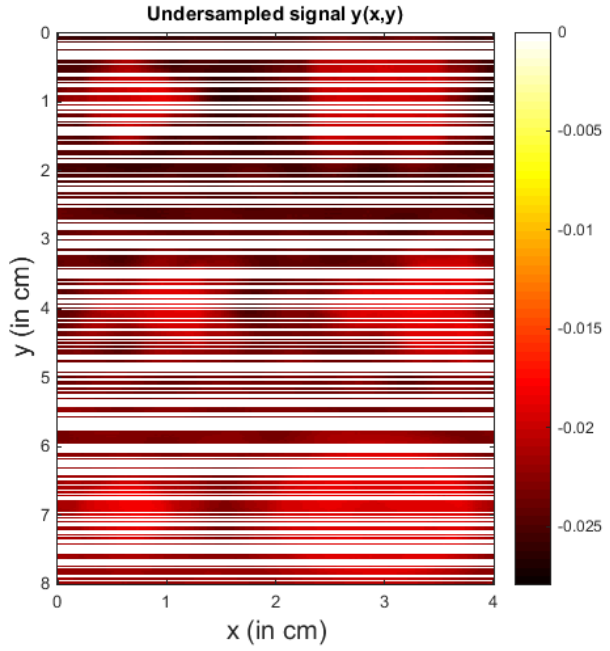

Fig.2.10. 50% Under-sampled Data

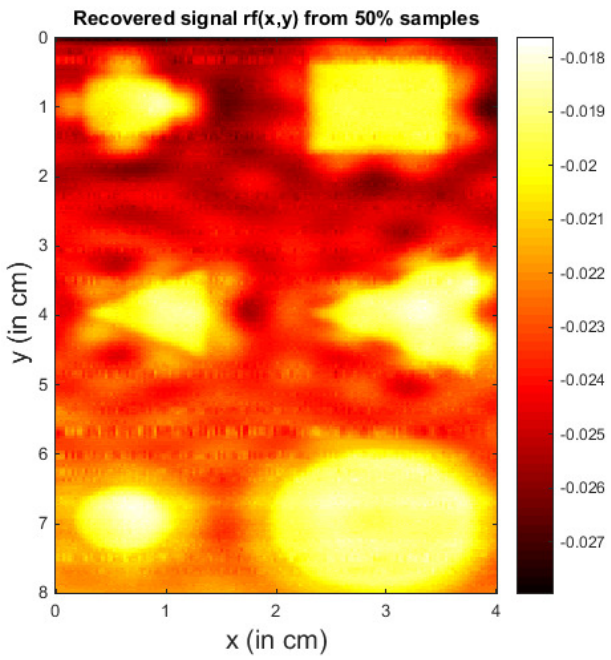

Fig.2.11 Recovered using orthogonal matching pursuit

Method 1 in Q2: The minimization using OMP algorithm is as follows:

The orthogonal matching pursuit algorithm tries to satisfy the error-constraints.

$$\mathrm{x} = \underset{x}{\operatorname{argmin}} \|x\| \, , such\ that\ \|y - Ax\|_2^2 \leq eps$$

where,

y is acquired undersampled signal

A is measurement dictionary

x is the sparse signal

The greedy-OMP selects the atoms with high correlation with current residual at each iteration (step 4) and projects the signal over the span of selected atoms.

$$\gamma = {A_I}^{+} res$$

which, can be solved by using Cholesky factorization and leads to practical implementation.

$$\gamma = (A_I' A_I) A_I' res$$

$A_I' A_I$ is a symmetric and positive definite matrix, which is updating with every iterations.

The cholesky factorization is simply represented as $R'R = A_I' A_I$, where R is the upper triangular matrix.

\\ Implemented Algorithm Steps:

1. Set, $x = 0 \; and \; res \leftarrow y$
2. $iter = 0$
3. **while,** $\|\boldsymbol{res}\| > \boldsymbol{eps}$ **, do**
4. $\hat{\imath} := argmax_i |A_i' res|$
5. $I = (I, \hat{\imath})$
6. find, $cholesky \; factorization \; R \; of \; A_i' A_i$
7. $\gamma := Solve \; for \; c \; \{RR^T c = A_i' res\}$
8. $res = y - A_I \gamma_I$
9. $iter = iter + 1$
10. **end while**

The minimization problem could have number of minima's available; reaching to global minimum is always hard. Using different minimization techniques and different set of constraints results in variation of finding minima. Orthogonal Matching Pursuit algorithm is leading the solution to one of its local minima or a limit point. The thought of finding other minima's with different constraints could have lead us to better solution, so one more minimization algorithm is applied to the same problem with different formulation of constraints called Proximal Gradient Algorithm [2]. The results are shown in Fig. 2.12.

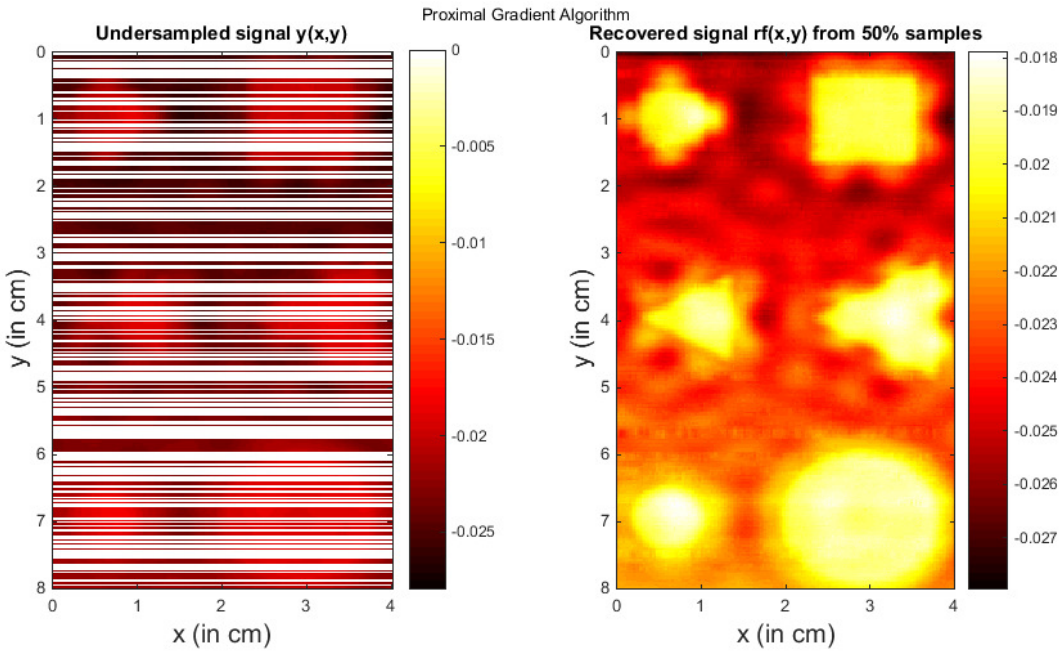

Fig.2.12 Results from Proximal Gradient Method

Method 2 in Q2: The minimization using Proximal Gradient Algorithm is as follows:

The orthogonal matching pursuit algorithm tries to satisfy the error-constraints.

$$\min_x \frac{1}{2}\|Ax - y\|_2^2 + \mu\|x\|_1$$

where,

y is acquired undersampled signal

A is measurement dictionary

x is the sparse signal

\\ Implemented Algorithm Steps:

1. Set, $\mu > 0, t = 1, \tau = eigenvalue\ of\ A'A$
2. $iter = 0$
3. **while,** $\|\boldsymbol{Ax} - \boldsymbol{y}\| > \boldsymbol{eps}$ **, do**

4. $Y^{iter} = X^{iter} + \frac{t^{iter-1}-1}{t^{iter}}\left(X^{iter} - X^{iter}\right)$
5. $Set, G^{iter} = Y^{iter} - \tau^{iter^{-1}} A^{*}(AY^{iter} - b)$
6. $Set, X^{iter+1} = S_{\tau^{iter}} G^{iter}$
7. $Compute\ t^{iter+1} = \frac{1+\sqrt{1+4\left(t^{iter}\right)^{2}}}{2}$
8. $iter = iter + 1$
9. **end while**

References:

1. R. Rubinstein, M. Zibulevsky and M Elad, "Efficient Implementation of the K-SVD Algorithm using Batch Orthogonal Matching Pursuit ", CS-2008.

2. K Toh, S. Yun "An accelerated proximal gradient algorithm for nuclear norm regularized least squares problems", NU-2009.

Description of any Problems/Challenges

The project progress is satisfactory according to the schedule of tasks table. Good communications between the PIs, students and program director is well maintained. No technical challenges were identified in this quarter.

Planned Activities for the Next Quarter

Besides the planned activities mentioned above, here are the future work for the next quarter Q3: ASU will continue the testing for material property characterization and Bayesian inference. Numerical simulation and experimental testing for ABI method will be further investigated. CU will continue to improve the sensitivity and resolution of the micro-electromagnetic imaging techniques assisted by multi-physics modeling. Pipe steel samples investigation will be carried out in Q3.